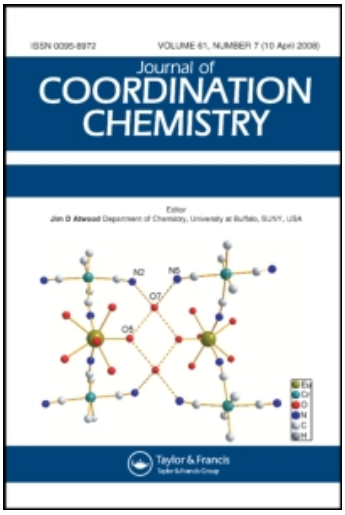

Journal of Coordination Chemistry
Publication details, including instructions for authors and subscription information:
http://www.informaworld.com/smpp/title~content=t713455674

Synthesis and characterization of a hydrazone ligand containing antipyrine and its transition metal complexes

Mohammad F. R. Fouda[a]; Mokhles M. Abd-Elzaher[a]; Mohamad M. Shakdofa[a]; Fathy A. El-Saied[b]; Mohammed I. Ayad[b]; Abdou S. El Tabl[b]
[a] Inorganic Chemistry Department, National Research Center, Cairo, Egypt [b] Faculty of Science, Department of Chemistry, Shebin El-Kom, Egypt

To cite this Article Fouda, Mohammad F. R. , Abd-Elzaher, Mokhles M. , Shakdofa, Mohamad M. , El-Saied, Fathy A. , Ayad, Mohammed I. and El Tabl, Abdou S.(2008) 'Synthesis and characterization of a hydrazone ligand containing antipyrine and its transition metal complexes', Journal of Coordination Chemistry, 61: 12, 1983 — 1996
To link to this Article: DOI: 10.1080/00958970701795714
URL: http://dx.doi.org/10.1080/00958970701795714

Journal of Coordination Chemistry
Vol. 61, No. 12, 20 June 2008, 1983–1996

Taylor & Francis
Taylor & Francis Group

Synthesis and characterization of a hydrazone ligand containing antipyrine and its transition metal complexes

MOHAMMAD F. R. FOUDA*†, MOKHLES M. ABD-ELZAHER†, MOHAMAD M. SHAKDOFA†, FATHY A. EL-SAIED‡, MOHAMMED I. AYAD‡ and ABDOU S. EL TABL‡

†Inorganic Chemistry Department, National Research Center, Dokki P.O. 12622, Cairo, Egypt
‡Faculty of Science, Department of Chemistry, El-Menoufia University, Shebin El-Kom, Egypt

(*Received 28 May 2007; in final form 26 June 2007*)

The coordination chemistry of N′-((1,5-dimethyl-3-oxo-2-phenyl-2,3-dihydro-1H-pyrazol-4-yl)methylene)-2-hydroxybenzohydrazide with copper(II), nickel(II), cobalt(II), manganese(II), zinc(II), palladium(II), iron(III), ruthenium(III), uranyl(VI), and titanium(IV) has been studied. The ligand and its complexes was characterized by elemental and thermal analyses, magnetic moments and conductivity measurements as well as spectroscopic techniques such as infrared, mass spectra, nuclear magnetic resonance, electron spin resonance and electronic absorption spectra. The spectral data showed that the ligand is monobasic tridentate coordinated via the enolic carbonyl oxygen of the hydrazide moiety, azomethine nitrogen and pyrazolone oxygen atoms.

Keywords: Synthesis; Hydrazone; Characterization; ESR; Transition metals; Complexes

1. Introduction

Hydrazones are a versatile class of ligands that have extensive applications in various fields, possessing pronounced biological and pharmaceutical activities as antitumor [1–3], antimicrobial [4], antituberculosis [5] and antimalarial agents [6]. Hydrazones play an important role in improving the antitumor selectivity and toxicity profile of antitumor agents by forming drug carrier systems employing suitable carrier proteins [7]. They also have anti-inflammatory and analgesic activity equal or close to that of aspirin [8, 9]. Hydrazones, such as pyridoxal isonecotinoylhydrazone, salicylaldehyde benzoylhydrazone and 2-pyridylcarboxaldehyde-2-thiophene carboxaldehyde hydrazone, act as orally effective drugs for treatment of iron overload diseases or genetic diseases β-thalassemia [10, 11]. Metal complexes of hydrazones have found applications in various chemical processes like nonlinear optics, sensors, etc. [12], and have been used in the separation and concentration of palladium and platinum in road dust [13].

*Corresponding author. Email: mfrfouda@yahoo.com

ISSN 0095-8972 print/ISSN 1029-0389 online © 2008 Taylor & Francis
DOI: 10.1080/00958970701795714

The present article was directed to preparation of copper(II), nickel(II), cobalt(II), manganese(II), zinc(II), palladium(II), iron(III), ruthenium(III), uranyl(VI), and titanium(IV) complexes with a new ligand N′-((1,5-dimethyl-3-oxo-2-phenyl-2,3-dihydro-1H-pyrazol-4-yl)methylene)-2-hydroxybenzohydrazide. The ligand and its complexes were characterized using various spectroscopic techniques such as infrared, mass spectra, nuclear magnetic resonance, electronic absorption spectra, electron spin resonance, and magnetic moment measurements as well as elemental and thermal analyses.

2. Experimental

The starting chemicals were of analytical grade and provided from Merck Company (Darmstadt, Germany). IR spectra of the ligand and complexes were recorded on a Perkin-Elmer infrared spectrometer 681 or Perkin-Elmer 1430 using KBr discs. The ^{1}H NMR spectra were recorded with a JEOL EX-270 MHz or JEOL ECA-500 MHz FT-NMR spectrometer in d_6-DMSO, where the chemical shifts were determined relative to the solvent peaks. The mass spectra of the ligand and its metal complexes were recorded using a JEOL JMS-AX-500 mass spectrometer provided with a data system. The molar conductivity of the metal complexes in DMSO at 10^{-3} M concentration were measured using a dip cell and a Bibby conductimeter MC1 at room temperature. The resistance is measured in Ohms, whereas the molar conductivities were calculated according to the equation $\Lambda = V \times K \times M_w/g \times \Omega$, where Λ = molar conductivity ($Ohm^{-1}cm^2mol^{-1}$), V = volume of the solution, K = cell constant 0.92 cm^{-1}, M_w = molecular weight of the complex, g = weight of the complex and Ω = resistance measured in Ohms. The electronic absorption spectra were recorded on a Shimadzu 240 or Perkin-Elmer 550 spectrometer using 1-cm quartz cells taking DMSO as solvent. The nujol mull electronic absorption spectra were recorded using Whatman filter paper No. 1 and referenced against similar filter paper saturated with paraffin oil. The magnetic susceptibilities of the polycrystalline complexes were measured in a borosilicate tube with a Johnson Matthey magnetic susceptibility balance at room temperature using the modified Gouy method [14]. The TGA were carried out on a Shimadzu DT-30 thermal analyzer in air from 27 to 800°C at a heating rate of 10°C per minute. The solid ESR spectra of the complexes were recorded with an ELEXSYS E500 Bruker spectrometer in 3-mm Pyrex Tubes at 298°K. Diphenylpicrylhydrazide (DPPH) was used as a g-marker for calibration of

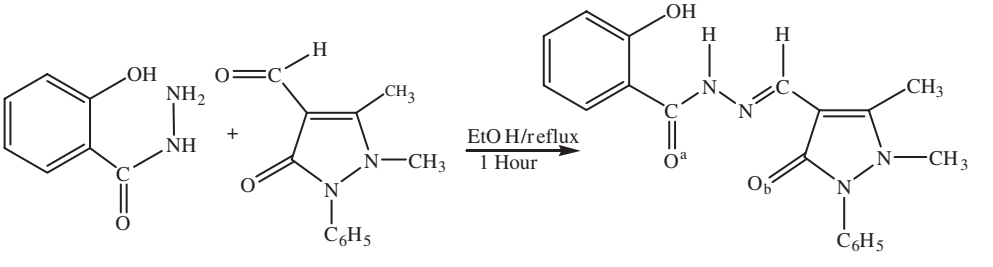

Figure 1. Preparation of the ligand.

the spectra. The elemental analyses (CHN) were performed in the Microanalytical Unit within Cairo University (Egypt) by the usual methods of analysis.

2.1. *Preparation of hydrazone ligand*

The hydrazone ligand was prepared by adding equimolar amounts of 2-hydroxybenzohydrazide (1 mmol in 20 mL of absolute ethanol) to 1,5-dimethyl-3-oxo-2-phenyl-2,3-dihydro-1H-pyrazole-4-carbaldehyde (1 mmol in 20 mL of absolute ethanol). The mixture was refluxed while stirring for one hour. The formed solid product was filtered off, washed with cold ethanol several times followed by crystallization from ethanol, and finally dried under vacuum.

2.2. *Preparation of metal complexes*

The metal complexes were prepared by adding equimolar amounts of salts of copper(II), nickel(II), cobalt(II), manganese(II), zinc(II), uranyl(VI), iron(III), titanium(IV) and ruthenium(III) (1 mmol in 20 mL of ethanol) to hydrazone ligand (1 mmol in 20 mL of ethanol) in the presence of 1 mmol triethylamine. The mixture was refluxed while stirring for four hours. The resulting solid complexes were filtered off, washed several times with ethanol, followed by drying under vacuum. The palladium complex was prepared by refluxing a mixture composed from a solution of 1 mmol of K_2PdCl_4 with 1 mmol of hydrazone ligand in absolute ethanol while stirring. The resulting orange precipitate was filtered off, washed with distilled water and ethanol, and dried under vacuum.

3. Results and discussion

The ligand, [N′-((1,5-dimethyl-3-oxo-2-phenyl-2,3-dihydro-1H-pyrazol-4-yl)methylene) -2-hydroxybenzohydrazide], H_2L and its metal complexes **1**–**22** were found to be stable at room temperature. The complexes were insoluble in common solvents such as ethanol, acetone, water and chloroform, but soluble in DMF as well as DMSO. The results of elemental analysis confirmed that all complexes are formed in 1 : 1 molar ratio between the metal and the ligand (table 1).

3.1. *Infrared spectra*

The infrared spectrum of H_2L showed a strong band at 1600 cm^{-1} assigned to $\nu(C{=}O^a)$ attached to the phenyl ring. This value may be lower than usual (ca. 1650 cm^{-1}) due to hydrogen bonding. The two weak bands at 3250 and 3150 cm^{-1} may be assigned to the ν(NH) [16, 17]. These findings indicate that the ligand is present in the ketonic form in the solid state [16]. The spectrum also showed two broad bands centered at 3445 and 2760 cm^{-1} may be assigned to the stretching vibration of the phenolic hydroxyl associated through intermolecular and intramolecular hydrogen bonding [16, 17]. The relatively strong bands located at 1643, 1588 and 1025 cm^{-1} are assigned to the

Table 1. The analytical and some physical characteristics for H_2L and its complexes.

No.	Ligand/complex	Color	B (°C)	M. Wt.	Calcd (Found)%			Λ^a_M	Yield (%)
					C	H	N		
1	H_2L ($C_{19}H_{18}N_4O_3$)	Yellowish white	211	350.4	65.1 (65.2)	5.2 (5.3)	16 (15.7)	–	95
2	$[Cu(HL)(CH_3COO)(H_2O)_2]\cdot H_2O$	Green	>300	526	48 (48.4)	5 (5.1)	10.7 (10.8)	11.2	70
3	$[Cu(HL)Cl(H_2O)_2]\cdot 2H_2O$	Green	280	520.4	43.9 (44.1)	4.8 (5)	10.8 (10.5)	13.8	72
4	$[Cu(HL)](NO_3)(H_2O)_2]$	Green	>300	511	44.7 (44.4)	4.1 (3.8)	13.7 (13.6)	22.7	75
5	$[Ni(HL)(CH_3COO)(H_2O)_2]\cdot 2H_2O$	Yellowish green	>300	539.2	46.8 (46.8)	5.2 (5.1)	10.4 (10.2)	16	65
6	$[Ni(HL)(Cl)(H_2O)_2]\cdot 2H_2O$	Brown	>300	515.6	44.3 (44.5)	4.9 (4.9)	10.9 (10.8)	27.1	75
7	$[Ni(HL)(NO_3)(H_2O)_2]$	Brown	>300	506.1	45.1 (44.6)	4.2 (4.4)	13.8 (13.4)	22.3	80
8	$[Co(HL)(CH_3COO)(H_2O)_2]\cdot 2H_2O$	Brown	>300	539.2	46.8 (46.5)	5.2 (4.4)	10.4 (10.1)	14.2	74
9	$[Co(HL)(Cl)(H_2O)_2]$	Brown	>300	479.5	47.6 (47.5)	4.4 (4.3)	11.7 (11.3)	16.5	69
10	$[Co(HL)(NO_3)(H_2O)_2]$	Brown	>300	506.1	45.1 (45.1)	4.2 (4.2)	13.8 (13.4)	13	65
11	$[Mn(HL)(CH_3COO)]$	Brown	>300	463.4	54.4 (54.3)	4.4 (4.5)	12. 1 (11.7)	12.3	70
12	$[Mn(HL)(Cl)](H_2O)$	Brown	>300	457.8	49.9 (50.2)	4.2 (4.2)	12.2 (11.9)	13.6	70
13	$[Zn(HL)(CH_3COO)]H_2O$	Yellowish white	>300	491.8	51.3 (51.2)	4.5 (4.7)	11.4 (11.1)	12.9	67
14	$[Zn(HL)(Cl)]H_2O$	Yellowish white	>300	468.2	48.7 (48.8)	4.1 (4.2)	12 (11.7)	15.1	60
15	$[Zn(L)(NO_3)]$	Yellowish white	>300	476.8	47.9 (48.1)	3.6 (3.5)	14.7 (14.5)	9.6	59
16	$[Fe(HL)Cl_2(H_2O)]$	Dark green	>300	494.1	46.2 (46.4)	3.9 (3.8)	11.3 (11)	22.3	55
17	$[Fe(HL)](NO_3)_2(H_2O)]\cdot H_2O$	Dark green	>300	565.3	40.4 (40.3)	3.7 (4)	14.9 (14.5)	18.3	57
18	$[UO_2(HL)(CH_3COO)]$	Yellow	>300	732.5	37.2 (37.2)	3 (3.2)	8.3 (8)	30.6	67
19	$[UO_2(HL)(NO_3)]\cdot 2H_2O$	Orange	>300	717.4	31.8 (32)	3 (3.4)	9.8 (9.5)	20.7	65
20	$[Ti(HL)Cl_3]$	Red orange	>300	503.6	45.3 (45.3)	3.7 (4)	10.3 (10.1)	21.5	50
21	$[Ru(HL)Cl_2\ (H_2O)]\cdot H_2O$	Dark brown	>300	539.4	42.3 (42.2)	3.8 (3.8)	10.4 (10.1)	17.2	75
22	$[Pd(HL)Cl]\cdot 2H_2O$	Yellowish orange	>300	527.3	43.3 (43.7)	4 (3.8)	10.6 (10.4)	24.3	63

[a]Molar conductivity as 10^{-3} M solutions ($Ohm^{-1}\,cm^2\,mol^{-1}$), B is the melting point or decomposition temperature.

ν(C=O^b) of the pyrazolone ring [18, 19], ν(C=N) of the azomethine group and ν(N-N), respectively [17].

The infrared spectra of the metal complexes **2**–**22** are presented in table 2. By comparing the infrared spectra of **2**–**22** with the free ligand, it was concluded that in all complexes the bands characteristic to ν(NH) and ν(C=O^a) in the infrared spectrum of the free ligand disappeared in the complexes. The disappearance of these bands indicated that the ligand coordinated with the metal ions in its enolic form. This suggestion is supported by the appearance of two new bands in the ranges 1570–1598 cm^{-1} and 1522–1557 cm^{-1}, which may be assigned to the conjugated system ν(C=N-N=C) and ν(N=C–O^a), respectively [19]. This finding may be due to bonding of the ligand with the metal ions through the enolic deprotonated oxygen. The characteristic band of the azomethine group ν(C=N) was shifted to lower frequency compared to that of the free ligand by 28 to 66 cm^{-1}. This may be taken as evidence of coordination of the azomethine nitrogen with the metal [17]. The characteristic band of ν(N-N) shifted from 1025 cm^{-1} in the spectrum of the ligand to 1032–1059 cm^{-1} in the spectra of the complexes. Lowering of the C=N frequency and increasing the frequency of N-N confirmed that the azomethine nitrogen participated in coordination with the metal ions [17]. The pyrazolone ring ν(C=O^b) shifted to lower frequency compared to that of the free ligand by 2–56 cm^{-1}, indicating that the pyrazolone oxygen atom participated in coordination [18, 19]. The appearance of a new band in the ranges 561–652 cm^{-1} for **2**–**22** may be assigned to the covalent metal oxygen bond. Bands in the ranges 504–593 and 428–509 cm^{-1} were taken as indication of coordination between the metal ions and the oxygen and nitrogen, respectively [21, 22]. A new band in the range 303–371 cm^{-1} may be assigned to ν(M–Cl) in the chloro complexes **3**, **6**, **9**, **12**, **14**, **16** and **20**–**22** [21, 22]. The spectra of acetato complexes **2**, **5**, **8**, **11**, **13** and **18** showed two bands characteristic to the acetate group, the first in the range 1542–1566 cm^{-1} and the second in the range 1354–1400 cm^{-1} assigned to ν(C=O) and ν(C–O), respectively. The difference between these two bands is in the range 170–201 cm^{-1}, suggesting that the acetate coordinates unidentate with the metal ions [23, 24]. In the case of nitrato complexes **7**, **10**, **15**, **17** and **19**, a strong band in the range 1375–1384 cm^{-1}, as well as a weak band around 1288–1320 cm^{-1}, was assigned to unidentate nitrate [25]. In the case of uranyl complexes **18** and **19**, the strong band characteristic for ν_3(O=U=O) was found at 922 and 918 cm^{-1}, respectively [26].

The above results together with elemental analysis indicates monobasic tridentate ligand coordinated via the enolic carbonyl oxygen of the hydrazide moiety, azomethine nitrogen and pyrazolone oxygen atoms.

3.2. *^{1}H NMR spectra*

The ^{1}H NMR spectra of H_2L was measured at room temperature using d_6-DMSO as a solvent. The spectrum showed two isomers with two peaks for the hydroxyl group (13.85, 12.85 ppm) [27, 28], the N*H* group (12.3, 11.6 ppm) [16, 17] and the azomethine group (*H*–C=N) (8.35, 7.95 ppm) [16] (table 3). The peaks observed as multiple ones at 6.8–7.9 ppm can be assigned to the aromatic protons [18] and the signals observed at 3.3 ppm and 2.5 ppm are assigned to (N–C*H*$_3$) and (C–C*H*$_3$), respectively [18, 19].

The ^{1}H NMR spectrum confirms that the ligand exhibits the keto form only with no evidence for the presence of the enol form from the appearance of

Table 2. The IR spectral (cm^{-1}) assignments for H_2L and metal complexes.

No.	Ligand/complex	OH/H_2O	NH	C=O[a]	C=O[b]	C=N/C=N–N=C	N=C–O	N–N	Ac/NO_3	M–O	M–N	M–Cl
1	H_2L ($C_{19}H_{18}N_4O_3$)	3445(br)	3250,3150	1600	1643	1588	–	1025	–	–	–	–
2	$[Cu(HL)(CH_3COO)(H_2O)_2]\cdot H_2O$	3435(br)	–	–	1634	1590	1549	1040	1560,1400	637,593	483	–
3	$[Cu(HL)Cl(H_2O)_2]\cdot 2H_2O$	3429(br)	–	–	1640	1597	1552	1035	–	578,538	500	–
4	$[Cu(HL)](NO_3)(H_2O)_2]$	3425(br)	–	–	1640	1598	1551	1033	1377,1295	652,577	464	350
5	$[Ni(HL)(CH_3COO)(H_2O)_2]\cdot 2H_2O$	3422(br)	–	–	1629	1590	1533	1034	1560,1367	621,566	500	–
6	$[Ni(HL)(Cl)(H_2O)_2]\cdot 2H_2O$	3380(br)	–	–	1632	1593	1546	1039	–	649,579	509	371
7	$[Ni(HL)(NO_3)(H_2O)_2]$	3423(br)	–	–	1641	1594	1545	1035	1383,1303	615,589	437	–
8	$[Co(HL)(CH_3COO)(H_2O)_2]\cdot 2H_2O$	3419(br)	–	–	1629	1595	1531	1039	1557,1360	619,580	535	–
9	$[Co(HL)(Cl)(H_2O)_2]$	3434(br)	–	–	1627	1589	1550	1039	–	582,550	425	361
10	$[Co(HL)(NO_3)(H_2O)_2]$	3427(br)	–	–	1636	1595	1556	1037	1382,1288	581, 537	466	–
11	$[Mn(HL)(CH_3COO)]$	3429(br)	–	–	1632	1595	1527	1038	1566,1365	594,504	468	–
12	$[Mn(HL)(Cl)](H_2O)$	3424(br)	–	–	1630	1594	1543	1038	–	586,505	434	328
13	$[Zn(HL)(CH_3COO)]H_2O$	3404(br)	–	–	1620	1598	1551	1038	1555,1354	573,543	474	–
14	$[Zn(HL)(Cl)]H_2O$	3426(br)	–	–	1632	1591	1550	1033	–	581,510	453	361
15	$[Zn(L)(NO_3)]$	3425(br)	–	–	1635	1597	1551	1032	1375,1290	572,542	428	–
16	$[Fe(HL)Cl_2(H_2O)]$	3423(br)	–	–	1626	1570	1552	1039	–	583,520	435	341
17	$[Fe(HL)](NO_3)_2(H_2O)]\cdot H_2O$	3426(br)	–	–	1621	1591	1546	1033	1382,1311	593,549	453	–
18	$[UO_2(HL)(CH_3COO)]$	3407(br)	–	–	1628	1582	1533	1034	1543,1373	561,529	474	–
19	$[UO_2(HL)(NO_3)]\cdot 2H_2O$	3427(br)	–	–	1634	1587	1552	1037	1382,1320	599,562	480	–
20	$[Ti(HL)Cl_3]$	3421(br)	–	–	1628	1589	1553	1036	–	586,515	458	303
21	$[Ru(HL)Cl_2(H_2O)]\cdot H_2O$	3440(br)	–	–	1615	1593	1522	1059	–	582,540	435	369
22	$[Pd(HL)Cl]\cdot 2H_2O$	3427(br)	–	–	1621	1590	1540	1041	–	583,530	445	303

C=O[a] is the carbonyl of the hydrazide moiety; C=O[b] is the carbonyl of the pyrazolone ring.

Table 3. ^{1}H NMR data for H_2L and its uranyl complex.

Groups	Signals (ppm)	
	Ligand	$[UO_2(HL)(CH_3COO)]$
ν(OH)	13.85, 12.85 (s, 1H)	12.78 (s, 1H)
ν(NH)	12.3, 11.6 (s, 1H)	–
ν(H–C=N)	8.35, 7.9 (s, 1H)	9.36 (s, 1H)
ν(Aromatic protons)	6.8–7.85 (m, 9H)	6.56–7.86 (m, 9H)
V(N–CH_3)	3.3 (s, 3H)	3.33 (s, 3H)
V(C–CH_3)	2.5 (s, 3H)	2.55 (s, 3H)

Table 4. Mass spectral data for H_2L.

Ligand	M/e	Relative intensity	Fragment
H_2L	350	100	$C_{19}H_{18}N_4O_3$
	243	90	$C_{13}H_{15}N_4O$
	213	57	$C_{12}H_{11}N_3O$
	199	33	$C_{12}H_{11}N_2O$
	188	27	$C_{11}H_{11}N_2O$
	111	40	$C_5H_7N_2O$
	104	95	C_7H_4O
	77	62	C_6H_5

NH and the absence of OH of the enolic form. Comparing the ^{1}H NMR spectrum of the ligand and that of **18** (table 3), the signal of NH disappeared indicating that the ligand coordinated to the metal in its enolic form. The signal characteristic to the phenolic hydroxyl group appeared in the same position indicating that the hydroxyl group did not participate in coordination [27]. Complexation leads to a significant downfield shift of the azomethine proton signal (9.36 ppm) relative to the free ligand indicating that the azomethine nitrogen atom coordinates to the metal ($N \rightarrow M$) [28].

3.3. *Mass spectra*

The mass spectrum of H_2L supported the suggested structure of the ligand, revealing a molecular ion peak m/z at 350, consistent with the molecular weight of the ligand. Moreover, the fragmentation pattern splits a parent ion peak at $m/z = 104$ corresponding to C_7H_4O, while the fragments at $m/z = 243$, 213, 199, 188, 111 and 77 correspond to $C_{13}H_{15}N_4O$, $C_{12}H_{11}N_3O$, $C_{12}H_{11}N_2O$, $C_{11}H_{11}N_2O$, $C_5H_7N_2O$, C_6H_6O and C_6H_5, respectively (table 4).

3.4. *Molar conductivity*

The molar conductivities of 1×10^{-3} M solutions of the metal complexes in DMSO at room temperature vary between 9.6 and 30.6 $Ohm^{-1}\,cm^2\,mol^{-1}$ (table 1). These values are indication of the non-electrolytic nature of **2**–**22**; high conductance values for some complexes may be due to partial solvolysis [29, 30].

3.5. *Electronic absorption spectra and magnetism*

The electronic absorption spectrum of the ligand exhibits five bands, 265, 310, 320, 350 and 380 nm. The first band at 265 nm may be attributed to $\pi \rightarrow \pi^*$ transition of the benzenoid moiety of the ligand, whereas the second band at 310 nm may be attributed to intraligand $\pi \rightarrow \pi^*$ transition. The third band at 320 nm may be attributed to hydrogen bonding and the last two bands at 350 and 380 nm may be assigned to $n \rightarrow \pi^*$ transition of the azomethine and carbonyl groups. These bands shifted to lower energy on complexation indicating the participation of these groups in coordination with metal ions [17, 28].

The electronic absorption spectra of copper(II) complexes **2**, **3**, and **4** in the solid state as well as in DMSO solution were almost identical, where they showed one broad band in the range 660–700 nm which may be assigned to superimposed transitions $^2B_{1g} \rightarrow {}^2E_g$, $^2B_{1g} \rightarrow {}^2A_{1g}$ and $^2B_{1g} \rightarrow {}^2B_{2g}$. The position as well as the broadness of this band indicate tetragonally distorted octahedral geometry around copper(II) (figure 2a) [31]. The magnetic moment values of the solid copper(II) complexes **2**, **3** and **4** at room temperature were 1.86, 1.78 and 1.9 B.M., respectively (table 5), consistent with the presence of one unpaired electron.

The electronic absorption spectra of the nickel(II) complexes **5**, **6** and **7** in solid state as well as in DMSO solution exhibit three bands, one in the range 915–965 nm which may be assigned to $^3A_{2g}(F) \rightarrow {}^3T_{2g}(F)$, the second in the range 645–670 nm may be assigned to $^3A_{2g}(F) \rightarrow {}^3T_{1g}(F)$ and the third in the range 410–430 nm may be assigned to $^3A_{2g}(F) \rightarrow {}^3T_{1g}(P)$. These bands clarified that the complexes are tetragonally distorted octahedral (figure 2a) [32]. The magnetic moment values of the solid nickel(II) complexes at room temperature were 3.14, 2.82 and 2.92 B.M., respectively (table 5), in the normal range for six-coordinate nickel(II).

The electronic absorption spectra of the cobalt(II) complexes **8**, **9** and **10** in the solid state and in DMSO solution showed three bands in the ranges 945–990, 500–690 and 430–475 nm, assigned to $^4T_{1g}(F) \rightarrow {}^4T_{2g}(F)$, $^4T_{1g}(F) \rightarrow {}^4A_{2g}(F)$, and $^4T_{1g}(F) \rightarrow {}^4T_{2g}(P)$, respectively. These findings suggest tetragonally distorted octahedral complexes (figure 2a) [33]. The magnetic moment values for cobalt(II) complexes at room temperature were in the range 4.39–4.77 B.M. (table 5).

The electronic absorption spectra of the manganese(II) complexes **11** and **12** showed no band in the visible region [34] due to the multiplicities of ground and excited states. The magnetic moments for manganese(II) complexes in the solid state at room temperature were 5.75 and 5.92 B.M., which correspond to five unpaired electrons in tetrahedral environment (figure 2b) [35].

The electronic absorption spectra of iron complexes **16** and **17** in solid state and in DMSO solutions showed two absorption bands in the ranges 610–630 and 460–470 nm. The relatively high intensity of these bands may be ascribed to borrowing of intensity from a low-lying charge transfer ligand band, because d-d transitions in iron(III) are forbidden. The bands indicate a tetragonally distorted octahedral geometry around iron(III) (figure 2c) [36], confirmed in the magnetic moments for **16** and **17** of 5.88 and 5.66 B.M., respectively (table 5), characteristic for high spin iron(III) complexes.

The electronic absorption spectrum of $[Ru(HL)Cl_2] \cdot 2H_2O$ in solid state and DMSO solutions showed only one band in the visible region at 580 nm ascribed to $^2T_{2g} \rightarrow {}^2A_{2g}$; a second band at 460 nm is assigned to charge transfer. These transitions indicate an octahedral ruthenium(III) complex (figure 2c) [37]. The magnetic moment obtained at

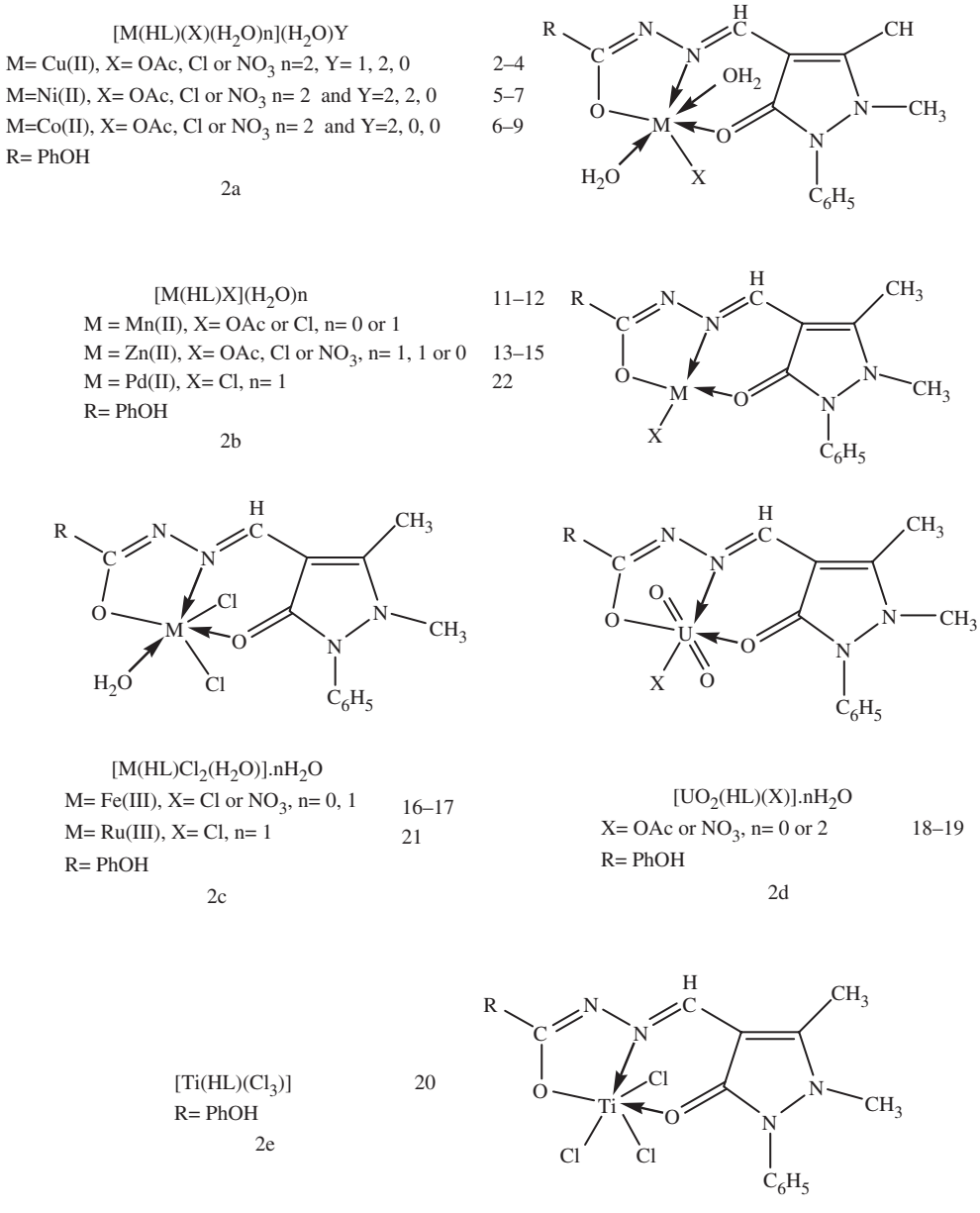

Figure 2. Structural representation of the complexes.

room temperature was 1.78 B.M. (table 5), corresponding to one unpaired electron suggesting a low spin ruthenium(III) in an octahedral environment.

The electronic absorption spectra of the uranyl complexes **18** and **19** in solid and in DMSO exhibit two bands, 460–500 nm and 420–440 nm. The higher energy band is assigned to charge transfer from uranyl oxygen to f-orbital of the uranium(VI) ion. The broadness of this band indicates unequal energies of the O → U charge transfer in the

Table 5. The electronic absorption spectra and magnetic moments for H_2L and its complexes.

No.	Ligand/complex	Bands in solid state	Bands in DMSO	μ_{eff} (B.M.)
1	H_2L ($C_{19}H_{18}N_4O_3$)	380, 350, 320, 310, 265	370, 350, 320, 305, 260	
2	$[Cu(HL)(CH_3COO)(H_2O)_2]\cdot H_2O$	660, 380, 355, 320, 310, 260	700, 380, 350, 320, 300, 265	1.86
3	$[Cu(HL)Cl(H_2O)_2]\cdot 2H_2O$	670, 375, 345, 310, 255	690, 375, 355, 340, 315, 300, 260	1.78
4	$[Cu(HL)](NO_3)(H_2O)_2]$	660, 380, 350, 320, 260	695, 380, 355, 340, 325, 300, 260	1.9
5	$[Ni(HL)(CH_3COO)(H_2O)_2]\cdot 2H_2O$	935, 660, 420, 380, 340, 310, 260	925, 670, 430, 385, 370, 350, 340, 310, 260	3.14
6	$[Ni(HL)(Cl)(H_2O)_2]\cdot 2H_2O$	920, 650, 420, 380, 340, 310, 260	915, 655, 420, 375, 350, 340, 315, 260	2.52
7	$[Ni(HL)(NO_3)(H_2O)_2]$	965, 650, 410, 375, 340, 310, 260	955, 645, 410, 380, 350, 340, 310, 260	2.58
8	$[Co(HL)(CH_3COO)(H_2O)_2]\cdot 2H_2O$	945, 580, 440, 380, 350, 320, 260	960, 600, 450, 375, 355, 320, 260	4.39
9	$[Co(HL)(Cl)(H_2O)_2]$	975, 690, 580, 430, 375, 350, 340, 320, 260	990, 650, 550, 475, 375, 355, 340, 320, 260	4.77
10	$[Co(HL)(NO_3)(H_2O)_2]$	990, 540, 460, 380, 355, 320, 260	985, 500, 450, 385, 355, 320, 265	4.43
11	$[Mn(HL)(CH_3COO)]$	400, 360, 340, 320, 260	395, 355, 330, 310, 260	5.75
12	$[Mn(HL)(Cl)](H_2O)$	400, 355, 330, 310, 260	390, 360, 330, 310, 265	5.92
13	$[Zn(HL)(CH_3COO)]H_2O$	380, 350, 320, 260	375, 355, 330, 310, 260	Dia.
14	$[Zn(HL)(Cl)]H_2O$	375, 350, 320, 260	375, 350, 325, 315, 260	Dia.
15	$[Zn(L)(NO_3)]$	410, 380, 320, 260	410, 375, 330, 310, 260	Dia.
16	$[Fe(HL)Cl_2(H_2O)]$	620, 460, 380, 350, 320, 255	610, 460, 370, 360, 330, 310, 255	5.88
17	$[Fe(HL)](NO_3)_2(H_2O)]\cdot H_2O$	630, 470, 380, 350, 320, 255	615, 460, 390, 360, 330, 315, 260	5.66
18	$[UO_2(HL)(CH_3COO)]$	470, 440, 380, 350, 330, 260	460, 430, 380, 355, 340, 310, 260	Dia.
19	$[UO_2(HL)(NO_3)]\cdot 2H_2O$	500, 430, 375, 340, 320, 260	480, 420, 370, 350, 330, 260	Dia.
20	$[Ti(HL)Cl_3]$	400, 380, 360, 320, 260	400, 375, 360, 345, 330, 310, 260	Dia.
21	$[Ru(HL)Cl_2(H_2O)]\cdot H_2O$	560, 480, 380, 340, 320, 260	580, 460, 370, 355, 340, 310, 255	1.78
22	$[Pd(HL)Cl]\cdot 2H_2O$	385, 350, 330, 300, 260	380, 350, 335, 310, 260	Dia.

Table 6. ESR parameters for some complexes.

No.	Complexes	$g_{\parallel}$	$g_{\perp}$	[a]g_{iso}	[b]G
2	$[Cu(HL)(CH_3COO)(H_2O)_2]$			2.095	
3	$[Cu(HL)Cl(H_2O)_2]\cdot 2H_2O$	2.20	2.03	2.087	6.7
4	$[Cu(HL)](NO_3)(H_2O)_2]$	2.207	2.025	2.086	8.3
11	$[Mn(HL)(CH_3COO)]$			2.02	
12	$[Mn(HL)(Cl)](H_2O)$			2.03	
16	$[Fe(HL)Cl_2(H_2O)]$	1.850	3.4	5.9	
17	$[Fe(HL)](NO_3)_2(H_2O)]\cdot H_2O$	1.8	4	3.27	
21	$[Ru(HL)Cl_2(H_2O]\cdot H_2O$	1.9	2.27	2.15	

[a]$g_{iso} = (2g_{\perp} + g_{\parallel})/3$, [b]$G = (g_{\parallel} - 2)/(g_{\perp} - 2)$.

two oxo cations. The band in the range 420–440 nm is assigned to charger transfer from ligand to the uranium(VI) ion [26].

3.6. *Electron spin resonance of copper(II), nickel(II), cobalt(II), manganese(II), iron(III) and ruthenium(III) complexes*

The ESR spectra of the copper(II) complexes **2**–**4** were recorded in polycrystalline state at room temperature. The spectrum of **2** showed an unresolved isotropic signal at high field. The isotropic g value of the complex is 2.095 [38]. The ESR spectra of **3** and **4** exhibited anisotropic signals with g values $g_{\parallel} = 2.2$ and 2.207; $g_{\perp} = 2.03$ and 2.025, respectively (table 6), characteristic for a d^9 system with axial symmetry and $d_{x^2-y^2}$ ground state. The $g_{\parallel}$ and $g_{\perp}$ values close to **2** and $g_{\parallel} > g_{\perp}$ (table 6) indicate tetragonal distortion around the copper(II) corresponding to elongation along the four-fold symmetry Z-axis. The trend $g_{\parallel} > g_{\perp} > g_e$ (2.0023) shows that the unpaired electron is localized in the $d_{x^2-y^2}$ orbital [39, 40]. Exchange coupling between two copper(II) ions is explained by the Hathaway expression $G = (g_{\parallel} - 2)/(g - 2)$. If $G > 4.0$ the exchange interaction is negligible, which is the case for **3** and **4** ($G = 6.7$ and 8.3) [39, 40]. Kivelson and Neiman noted that for an ionic environment, g is normally 2.3 or larger, but for covalent environment $g_{\parallel}$ is less than 2.3. The $g_{\parallel}$ value for **3** and **4** are 2.2 and 2.207, respectively, indicating a significant degree of covalency in the metal–ligand bond [39, 40].

The ESR spectra of the solid cobalt(II) and nickel(II) complexes at room temperature do not show a signal due to rapid spin lattice relaxation of cobalt(II) and nickel(II) broadening the lines [41].

The ESR spectra of the manganese(II) complexes **11** and **12** at room temperature give one broad isotropic signal at 2.02 and 2.03, respectively, indicating tetragonally distorted complexes with spin orbit coupling. This leads to short relaxation times, where absorption is difficult to observe [38, 39, 41].

The ESR spectra of **16** at room temperature showed three bands at 1.85, 3.4 and 6.0. These values represent the signal of high spin iron(III) ($S = 5/2$) and low spin iron(III) ($S = 1/2$) indicating the presence of both high and low spin states of iron(III) within the crystal lattice, where the ESR signal results from the interaction between the high spin Fe(III) ($S = 5/2$) and low spin Fe(III) ($S = 1/2$) [42]. The ESR spectrum of **17** was

Table 7. The thermal analysis (TGA) of some complexes.

No.	Complexes	Temp. range (°C)	Loss in weight found (calculated)	Assignment	Composition of the residue
		27–80	3.3 (3.4)	Dehydration process (H_2O)	$[Cu(HL)(CH_3COO)(H_2O)_2]$
2	$[Cu(HL)(CH_3COO)(H_2O)_2]\cdot H_2O$	82–175	6.67 (6.84)	Loss of two molecule of coordinated water	$[Cu(HL)(CH_3COO)]$
		176–280	11.7 (11.4)	Loss of one acetate group	[Cu(HL)]
		290–780	67.8 (66.5)	Decomposition of the complex forming CuO	CuO
3	$[Cu(HL)Cl(H_2O)_2]\cdot 2H_2O$	23–130	6.5 (6.2)	Dehydration process ($2H_2O$)	$[Cu(HL)Cl(H_2O)_2]$
		130–265	7.3 (6.9)	Loss of two molecule of coordinated water	[Cu(HL)Cl]
		265–315	7.3 (6.8)	Loss of one chloride ion (HCl)	[Cu(HL)]
		315–596	69.1 (67.1)	Decomposition of the complex forming CuO	CuO
5	$[Ni(HL)(CH_3COO)(H_2O)_2]\cdot 2H_2O$	23–75	7 (6.68)	Dehydration process ($2H_2O$)	$[Ni(HL)(OAc)(H_2O)_2]$
		75–180	6.54 (6.68)	Loss of two molecule of coordinated water	[Ni(HL)(OAc)]
		180–300	11.2 (11.0)	Loss of one acetate group	[Ni(HL)]
		300–473	64.1 (64.7)	Decomposition of the complex forming NiO	NiO
6	$[Ni(HL)(Cl)(H_2O)_2]\cdot 2H_2O$	30–90	6.7 (7.0)	Dehydration process ($2H_2O$)	$[Ni(HL)(Cl)(H_2O)_2]$
		90–220	6.7 (7.0)	Loss of two molecule of coordinated water	[Ni(HL)(Cl)]
		220–330	7.2 (6.9)	Loss of one chloride ion (HCl)	[Ni(HL)]
		330–560	68.9 (68.1)	Decomposition of the complex forming NiO	NiO
8	$[Co(HL)(CH_3COO)(H_2O)_2]\cdot 2H_2O$	20–100	6.8 (6.7)	Dehydration process ($2H_2O$)	$[Co(HL)(OAc)(H_2O)_2]$
		100–230	7 (6.7)	Loss of two molecule of coordinated water	[Co(HL)(OAc)]
		230–325	11.4 (11)	Loss of one acetate group	[Co(HL)]
		325–370	62.5 (64.8)	Decomposition of the complex forming CuO	CoO
12	$[Mn(HL)(Cl)](H_2O)$	21–137	4.1 (3.94)	Dehydration process (H_2O)	[Mn(HL)(Cl)]
		138–305	7.95 (7.74)	Loss of one chloride ion (HCl)	[Mn(HL)]
		305–423	65.9 (71.2)	Decomposition of the complex forming MnO	Mn_2O_3
14	$[Zn(HL)(Cl)]H_2O$	23–124	4.3 (3.85)	Dehydration process (H_2O)	[Zn(HL)(Cl)]
		126–350	7.7 (7.57)	Loss of one chloride ion (HCl)	[Zn(HL)]
		350–506	69.2 (71.2)	Decomposition of the complex forming ZnO	ZnO
21	$[Ru(HL)Cl_2(H_2O)]\cdot H_2O$	37–110	3.65 (3.33)	Dehydration process (H_2O)	$[Ru(HL)Cl_2(H_2O)]$
		110–196	3.65 (3.33)	Loss of one molecule of coordinated water	$[Ru(HL)Cl_2]$
		200–260	13 (13.1)	Loss of two chloride ion (HCl)	[Ru(HL)]
		260–415	64.2 (31.4)	Decomposition of the complex forming Ru_2O_3	Ru_2O_3

different from **16**, with two signals at g values 1.8 and 4.0, from iron(III) doped distorted media in a weak crystal field. In the case of the present iron(III) complex, the $^6A_1$ ground state is spilt into three Kramer's doublets due to spin-orbit mixing with excited states. These doublets are split by an applied magnetic field and the near isotropic g-factor of 4.0 is assigned to a transition within one of them [43].

The ESR of ruthenium complex **21** was recorded at room temperature and the g values are given in table 6. The low spin d^5 configuration is a good probe of molecular structure and bonding since the observed g values are very sensitive to small changes in the structure and to metal ligand covalency. The ESR spectrum of this complex exhibits characteristics of an axially-symmetric system with $g_{\|}$ at 1.9 and $g_{\perp}$ at 2.27 for an octahedral field with tetragonal distortion [37].

3.7. *Thermal analyses of some complexes*

The thermal analyses (TGA) was carried out on **2**, **3**, **5**, **6**, **8**, **12**, **14** and **21** in the temperature range 20–800°C and the results are collected in table 7, showing good agreement in weight loss between calculated and the found formulae. The thermal analyses showed that **2**, **3**, **5**, **6**, **8**, **12**, **14** and **21** generally decomposed in several steps. The first step (23–137°C) for all complexes represented dehydration. The second step (75–265°C) only observed for **2**, **3**, **5**, **6, 8** and **21** may be assigned to elimination of coordinated water. The third step (126–375°C) for all complexes is the elimination of the chloride or acetate. The fourth step (290–780°C) is complete decomposition of the complexes ending with metal oxide formation.

The elemental analysis, IR, ^{1}H NMR, mass and electronic spectra, and magnetic moment measurement, as well as the electron spin resonance and thermal analyses are compatible with the proposed structures (figure 2).

References

[1] N. Terzioglu, A. Gürsoy. *Eur. J. Med. Chem.*, **38**, 781 (2003).
[2] M.T. Cocco, C. Congiv, V. Lilliu, V. Onnis. *Bioorg. Med. Chem.*, **14**, 366 (2006).
[3] J. Easmon, G. Pverstinger, G. Heinish, J. Hofmann. *Int. J. Cancer*, **94**, 89 (2001).
[4] P. Vicini, F. Zani, P. Cozzini, I. Doytchinova. *Eur. J. Med. Chem.*, **37**, 553 (2002).
[5] J. Patole, U. Sandbhor, S. Padhye, D.N. Deobagkar, C.E. Anson, A. Powell. *Bioorg. Med. Chem. Lett.*, **13**, 51 (2003).
[6] A. Walcourt, M. Loyevsky, D.B. Lovejoy, V.R. Gordeuk, D.R. Richardson. *Int. J. Biochem. Cell Biol.*, **36**, 401 (2004).
[7] F. Kratz, U. Beyer, T. Roth, N. Tarasova, P. Collery, F. Lechenault, A. Cazabat, P. Schumacher, C. Unger, U. Falken. *J. Pharm. Sci.*, **87**, 338 (1998).
[8] S.M. Sondhi, M. Dinodia, A. Kumar. *Bioorg. Med. Chem.*, **14**, 4657 (2006).
[9] T.M. Aminabhavi, N.S. Birader, C.S. Patil. *Inorg. Chim. Acta*, **78**, 107 (1983).
[10] T.B. Chaston, D.R. Richardson. *Amer. J. Hematol.*, **73**, 200 (2003).
[11] P.V. Bernhardt, P. Chin, P.C. Sharpe, J.-Y.C. Wang, D.R. Richardson. *J. Biol. Inorg. Chem.*, **10**, 761 (2005).
[12] M. Bakir, I. Hassan, T. Johnson, O. Brown, O. Green, C. Gyles, M.D. Coley. *J. Mol. Struct.*, **688**, 213 (2004).
[13] X. Ge, I. Wender, P. Schramel, A. Kettrup. *React. Funct. Polym.*, **61**, 1 (2004).
[14] M. Massaccsi, R. Pinna, G. Poticelli. *Spectrochim. Acta, Part A*, **38**, 725 (1982).
[15] S. Das, S. Pal. *J. Mol. Struct.*, **753**, 68 (2005).
[16] O. Pouralimardan, A.-C. Chamayou, C. Janiak, H. Hosseini-Monfared. *Inorg. Chim. Acta*, **360**, 1599 (2006).

[17] R. Gup, B. Kirkan. *Spectrochim. Acta, Part A*, **62**, 1188 (2005).
[18] R.C. Maurya, S. Rajput. *J. Mol. Struct*., **833**, 133 (2007).
[19] K.Z. Ismail. *Transition Met. Chem*., **25**, 522 (2000).
[20] S. Yaocheng, S. Qingbao, W. Xiaoli, M. Yongxiang. *Polyhedron*, **13**, 2101 (1994).
[21] A. Tossidis, C.A. Bolos. *Inorg. Chim. Acta*, **112**, 93 (1986).
[22] B. Murukan, K. Mohanan. *Transition Met. Chem*., **31**, 441 (2006).
[23] K. Nakamoto., *Infrared and Raman Spectra of Inorganic and Coordination Compounds*, 3rd Edn, pp. 232–233, J. Wiley & Sons, New York (1994).
[24] L.K. Gupta, U. Bansal, S. Chandra. *Spectrochim. Acta, Part A*, **65**, 463 (2006).
[25] S. Ghosh, T.K. Bandyopadhyay. *Transition Met. Chem*., **10**, 57 (1985).
[26] J.B. Gandhi, N.D. Kulkarni. *Transition Met. Chem*., **25**, 209 (2000).
[27] H.D. Yin, S.W. Chen. *Inorg. Chim. Acta*, **359**, 3330 (2006).
[28] M.R. Maurya, S. Agarwal, C. Bader, D. Rehder. *Eur. J. Inorg. Chem*., 147 (2005).
[29] W.J. Geary. *Coord. Chem. Rev*., **7**, 81 (1971).
[30] K.K. Narang, V.P. Singh. *Transition Met. Chem*., **18**, 287 (1993).
[31] K.K. Narang, V.P. Singh. *Transition Met. Chem*., **21**, 507 (1996).
[32] N. Al-Awadi, N.M. Shuaib, A. El-Dissouky. *Spectrochim. Acta, Part A*, **65**, 36 (2006).
[33] G.G. Mohamed, N.E.A. El-Gamel. *Spectrochim. Acta, Part A*, **60**, 3141 (2004).
[34] K.B. Gudasi, M.S. Oatil, R.S. Vadavi, R.V. Shenoy, S.A. Patil, M. Nethaji. *Transition Met. Chem*., **31**, 580 (2006).
[35] M. Salavati-Niasari, A. Amiri. *Appl. Catal*., **290**, 46 (2005).
[36] G.M. Abu El-Reash, K.M. Ibrahim, M.M. Bekheit. *Transition Met. Chem*., **15**, 148 (1990).
[37] G. Venkatachalam, R. Ramesh. *Spectrochim. Acta, Part A*, **61**, 2081 (2005).
[38] K.B. Gudasi, S.A. Patil, R.S. Vadavi, R.V. Shenoy. *Transition Met. Chem*., **31**, 586 (2006).
[39] S. Chandra, L.K. Gupta. *Spectrochim. Acta, Part A*, **60**, 2411 (2004).
[40] S. Chandra, U. Kumar. *Spectrochim. Acta, Part A*, **60**, 2825 (2004).
[41] S. Chandra, U. Kumar. *Spectrochim. Acta, Part A*, **61**, 219 (2005).
[42] Y.-J. Sun, L. Yi, X. Yang, Y. Liu, P. Cheng, D.-Z Liao, S.-P. Yan, Y.-H. Jiang. *Inorg. Chim. Acta*, **358**, 396 (2005).
[43] D. Skrzypek, B. Szymanska, D. Kovala-Demertzi, J. Wiecek, E. Talik, M.A. Demertzis. *J. Phys. Chem. Solids*, **69**, 2550 (2006).